

1 Unveiling Crucivirus Diversity by Mining 2 Metagenomic Data

3 **Ignacio de la Higuera¹, George W. Kasun¹, Ellis L. Torrance¹, Alyssa A. Pratt¹,**
4 **Amberlee Maluenda¹, Jonathan Colombe², Maxime Bissex², Viviane Ravet²,**
5 **Anisha Dayaram³, Daisy Stainton⁴, Simona Kraberger⁵, Peyman Zawar-Reza⁶,**
6 **Sharyn Goldstien⁷, James V. Briskie⁷, Robyn White⁷, Helen Taylor⁸, Christopher**
7 **Gomez⁹, David G. Ainley¹⁰, Jon S. Harding⁷, Rafaela S. Fontenele⁵, Joshua**
8 **Schreck⁵, Simone G. Ribeiro¹¹, Stephen A. Oswald¹², Jennifer M. Arnold¹²,**
9 **François Enault², Arvind Varsani^{5,7,13} and Kenneth M. Stedman¹.**

10 ¹Department of Biology, Center for Life in Extreme Environments, Portland State University, P.O. Box
11 751, Portland, OR 97207-0751, USA

12 ²Université Clermont Auvergne, CNRS, Laboratoire Microorganismes: Génome et Environnement, UMR
13 6023, Clermont-Ferrand, France

14 ³Institut für Neurophysiology, Charité-Universitätsmedizin, Charitéplatz 1, Berlin 10117, Germany

15 ⁴Department of Entomology and Plant Pathology, Division of Agriculture, University of Arkansas
16 System, Fayetteville, AR 72701, USA

17 ⁵The Biodesign Center for Fundamental and Applied Microbiomics, Center for Evolution and Medicine,
18 School of Life Sciences, Arizona State University, Tempe, AZ 85287, USA

19 ⁶School of Earth and Environment, University of Canterbury, Christchurch, New Zealand

20 ⁷School of Biological Sciences, University of Canterbury, Private Bag 4800, Christchurch 8140, New
21 Zealand

22 ⁸Department of Anatomy, University of Otago, Lindo Ferguson Building, Great King Street, Dunedin,
23 9016, New Zealand

24 ⁹Graduate School of Maritime Sciences, Laboratory of Sediment Hazards and Disaster Risk, Kobe
25 University, Kobe City, Japan

26 ¹⁰HT Harvey and Associates, Los Gatos, CA 95032, USA

27 ¹¹Embrapa Recursos Genéticos e Biotecnologia, Brasília, DF 70770-017, Brazil

28 ¹²Division of Science, Pennsylvania State University, Berks Campus, Reading, PA 19619, USA

29 ¹³Structural Biology Research Unit, Department of Clinical Laboratory Sciences, University of Cape
30 Town, Rondebosch, Cape Town, South Africa

31 Correspondence should be addressed to Kenneth M. Stedman: kstedman@pdx.edu

32 **KEYWORDS:** Crucivirus, CRESS-DNA viruses, gene transfer, recombination, virus
33 evolution

34 ABBREVIATIONS

35 CruV: Crucivirus; CRESS: Circular Rep-Encoding Single Stranded; CP: Capsid; RdRP:
36 RNA-dependent RNA Polymerase; ORF: Open Reading Frame; SJR: Single Jelly Roll;
37 PI: Pairwise Identity; MDA: Multiple Displacement Amplification; S3H: Superfamily 3
38 helicase; RCR: Rolling Circle Replication; CDS: Coding Sequence; CruCGE: Cruciv-
39 like Circular Genetic Element

40 **ABSTRACT**

41 The discovery of cruciviruses revealed the most explicit example of a common protein
42 homologue between DNA and RNA viruses to date. Cruciviruses are a novel group of
43 circular Rep-encoding ssDNA (CRESS-DNA) viruses that encode capsid proteins (CPs)
44 that are most closely related to those encoded by RNA viruses in the family
45 *Tombusviridae*. The apparent chimeric nature of the two core proteins encoded by
46 crucivirus genomes suggests horizontal gene transfer of CP genes between DNA and
47 RNA viruses. Here, we identified and characterized 451 new crucivirus genomes and
48 ten CP-encoding circular genetic elements through *de novo* assembly and mining of
49 metagenomic data. These genomes are highly diverse, as demonstrated by sequence
50 comparisons and phylogenetic analysis of subsets of the protein sequences they encode.
51 Most of the variation is reflected in the replication associated protein (Rep) sequences,
52 and much of the sequence diversity appears to be due to recombination. Our results
53 suggest that recombination tends to occur more frequently among groups of cruciviruses
54 with relatively similar capsid proteins, and that the exchange of Rep protein domains
55 between cruciviruses is rarer than gene exchange. Altogether, we provide a
56 comprehensive and descriptive characterization of cruciviruses.

57 **IMPORTANCE**

58 Viruses are the most abundant biological entities on Earth. In addition to their impact on
59 animal and plant health, viruses have important roles in ecosystem dynamics as well as
60 in the evolution of the biosphere. Circular Rep-encoding single-stranded (CRESS) DNA
61 viruses are ubiquitous in nature, many are agriculturally important, and are viruses that
62 appear to have multiple origins from prokaryotic plasmids. CRESS-DNA viruses such
63 as the cruciviruses, have homologues of capsid proteins (CPs) encoded by RNA viruses.
64 The genetic structure of cruciviruses attests to the transfer of capsid genes between
65 disparate groups of viruses. However, the evolutionary history of cruciviruses is still
66 unclear. By collecting and analyzing cruciviral sequence data, we provide a deeper
67 insight into the evolutionary intricacies of cruciviruses. Our results reveal an unexpected
68 diversity of this virus group, with frequent recombination as an important determinant
69 of variability.

70 INTRODUCTION

71 In the last decade, metagenomics has allowed for the study of viruses from a
72 new angle; viruses are not merely agents of disease, but abundant and diverse members
73 of ecosystems (1, 2). Viruses have been shaping the biosphere probably since the origin
74 of life, as they are important drivers of the evolution of the organisms they infect (3–5).
75 However, the origin of viruses is not entirely clear. Viruses, as replicons and mobile
76 elements, are also subject to evolution. Virus variability is driven by various mutation
77 rates, recombination and reassortment of genetic components (6). These attributes,
78 coupled with types of genomes (RNA or DNA, single or double stranded and circular or
79 linear), lead to a large genetic diversity in the ‘viral world’.

80 Viruses are generally classified based on the nature of their transmitted genetic
81 material (7). Viral genetic information is coded in either RNA or DNA. Moreover, these
82 genomes can be single (positive or negative sense) or double stranded, linear or circular,
83 and can be comprised of a single or multiple molecules of nucleic acid (monopartite or
84 multipartite, respectively). These different groups of viruses have different replication
85 strategies, and they harbor distinct taxa based on their genome arrangement and
86 composition (1). The striking differences between viral groups with disparate genome
87 types suggest polyphyletic virus origins (8).

88 For example, the highly abundant circular Rep-encoding single-stranded DNA
89 (CRESS-DNA) viruses may have been derived from plasmids on multiple occasions by
90 acquiring capsid genes from RNA viruses (9–11). Eukaryotic CRESS-DNA viruses
91 constitute a diverse and widespread group of viruses with circular genomes –some of
92 them multipartite– that contains the families *Geminiviridae*, *Circoviridae*, *Nanoviridae*,
93 *Alphasatellitidae*, *Genomoviridae*, *Bacilladnaviridae*, *Smacoviridae* and
94 *Redondoviridae* (ICTV classification for some groups is pending at this time), in
95 addition to vast numbers of unclassified viruses (12, 13). Universal to all CRESS-DNA
96 viruses is the Rep, which is involved in the initiation of the virus’ rolling-circle
97 replication. Rep homologues are also encoded in plasmids (13, 14). Some pathogenic
98 CRESS-DNA viruses are agriculturally important, such as porcine circoviruses, and
99 nanoviruses and geminiviruses that infect a wide range of plant hosts (12). However,

100 many CRESS-DNA viruses have been identified in apparently healthy organisms, and
101 metagenomics have revealed their presence in most environments (12).

102 In 2012, a metagenomic survey of a hot and acidic lake in the volcanic Cascade
103 Range of the western USA uncovered a new type of circular DNA virus (15). The
104 genome of this virus is a CRESS-DNA virus based on the circularity of its sequence, the
105 presence of a *rep* gene, and a predicted stem-loop structure with a conserved nucleotide
106 sequence (*ori*) that serves as an origin for CRESS-DNA virus rolling-circle replication
107 (RCR; reviewed in (16, 17)). Interestingly, the sequence of CP encoded by this genome
108 resembles those encoded by the RNA viruses in the family *Tombusviridae* (15). It was
109 hypothesized that this virus originated by the acquisition of a capsid gene from an RNA
110 virus through a yet to be demonstrated RNA-DNA recombination event (15, 18). Since
111 the discovery of this putatively “chimeric virus”, 80 circular sequences encoding a Rep
112 and a CP that share homology to tombusvirus CPs have been found in different
113 environments around the globe (19, 20, 29–31, 21–28). This growing group of viruses
114 have been branded “cruciviruses”, as they imply the *crossing* between CRESS-DNA
115 viruses and RNA tombusviruses (27). Cruciviruses have been found associated with
116 forams (20), alveolates hosted by isopods (26), arthropods (19, 22), and in peatland
117 ecosystems (27), but no host for cruciviruses have been elucidated to date.

118 The circular genome of known cruciviruses is variable in size, ranging from 2.7
119 to 5.7 kb and often contains ORFs in addition to the Rep and CP, which have been
120 found in either a unisense or an ambisense orientation (20, 27). The function of
121 additional crucivirus ORFs is unclear due to the lack of sequence similarity with any
122 characterized protein. The genome replication of CRESS-DNA viruses is initiated by
123 the Rep protein, that binds to direct repeats present just downstream of the stem of the
124 *ori*-containing stem-loop structure and nicks the ssDNA (32, 33). The exposed 3'OH
125 serves as a primer for cellular enzymes to replicate the viral genome via RCR (33–35).
126 The exact terminating events of CRESS-DNA virus replication are poorly understood
127 for most CRESS-DNA viruses, but Rep is known to be involved in the sealing of newly
128 replicated genomes (33, 35–37).

129 Rep has a domain in the N-terminus that belongs to the HUH endonuclease
130 superfamily (38). This family of proteins is characterized by a HUH motif (Motif II), in
131 which two histidine residues are separated by a bulky hydrophobic amino acid, and a

132 Tyr-containing motif (Motif III) that catalyzes the nicking of the ssDNA (38–41).
133 CRESS-DNA virus Reps also contain a third conserved motif in the N-terminal portion
134 of the protein (Motif I), likely responsible for dsDNA binding specificity (42). In many
135 CRESS-DNA viruses, the HUH motif has been substituted for a similar motif that lacks
136 the second histidine residue (e.g. circoviruses have replaced HUH with HLQ) (10, 38).
137 The C-terminal portion of eukaryotic CRESS-DNA virus Reps contain a Superfamily 3
138 helicase domain (S3H) that may be responsible for unwinding dsDNA replicative
139 intermediates (43, 44). This helicase domain is characterized by Walker A and B motifs,
140 Motif C and an Arg finger. Previous studies have identified evidence of recombination
141 in the endonuclease and helicase domains of Rep, which contributes to the potential
142 ambiguity of Rep phylogenies (45). Interestingly, the Rep proteins of different
143 cruciviruses have been shown to be similar to CRESS-DNA viruses in different
144 families, including circoviruses, nanoviruses, and geminiviruses (20, 27). In some
145 cruciviruses, these differences in phylogeny have been observed between the individual
146 domains of a single Rep protein (21, 27). The apparent polyphyly of crucivirus Reps
147 suggests recombination events involving cruciviruses and other CRESS-DNA viruses,
148 even within Reps (20, 21).

149 All characterized CRESS-DNA viruses package their DNA into small capsids
150 with icosahedral symmetry or their geminate variants, built from multiple copies of the
151 CP encoded in their genome (12). The CP of these CRESS-DNA viruses appears to fold
152 into an eight-strand β -barrel that conforms to the single jelly-roll (SJR) architecture,
153 which is also commonly found in eukaryotic RNA viruses (46). The CP of cruciviruses
154 has no detectable sequence similarity with the capsid of other CRESS-DNA viruses, and
155 is predicted to adopt the SJR conformation found in the CP of tombusviruses (15, 20,
156 21). Three domains can be distinguished in tombusviral CPs (47, 48). From the N- to
157 the C-terminus: i) The RNA-interacting or R-domain, a disordered region that faces the
158 interior of the viral particle to interact with the nucleic acid through abundant basic
159 residues (49, 50), ii) the shell or S-domain containing the single jelly-roll fold and the
160 architectural base of the capsid (48) and iii) the protruding or P-domain, that decorates
161 the surface of the virion and is involved in host transmission (51). In tombusviruses, the
162 S-domain of 180 CP subunits interact with each other to assemble around the viral RNA
163 in a T=3 fashion, forming a $\varnothing\sim35$ nm virion (48, 52).

164 The study of cruciviruses suggests evidence for the transfer of capsid genes
165 between disparate viral groups, which can shed light on virus origins and the phenotypic
166 plasticity of virus capsids. Here, we document the discovery of 461 new crucivirus
167 genomes (CruV) and cruci-like circular genetic elements (CruCGE) identified in
168 metagenomic data obtained from different environments and organisms. This study
169 provides a comprehensive analysis of this greatly expanded dataset and explores the
170 extent of cruciviral diversity –mostly due to Rep heterogeneity– impacted by rampant
171 recombination.

172 **MATERIALS AND METHODS**

173 **Recovery of viral genomes from assembled viromes.**

174 A total of 461 crucivirus-related sequences were identified from 1168
175 metagenomic surveys (Supp. Tables 1 and 2). 1167 viromes from 57 published datasets
176 and one unpublished virome were obtained from different types of environments: i)
177 aquatic systems (freshwater, seawater, hypersaline ponds, thermal springs and
178 hydrothermal vents), ii) engineered systems (bioreactor, food production), and iii)
179 eukaryote-associated flora (human, insect and other animal feces, human saliva and
180 fluids, cnidarians and plants). New cruciviral sequences were identified in these viromes
181 by screening circular contigs for the presence of CPs from previously known
182 cruciviruses (20) and tombusviruses, using a BLASTx bit-score threshold of 50.

183 Additionally, sequences CruV-240, CruV-300, CruV-331, CruV-338 and CruV-
184 367 were retrieved from Joint Genome Institute (JGI)'s IMG/VR repository (53), by
185 searching scaffolds with a function set including the protein family pfam00729,
186 corresponding to the S-domain of tombusvirus capsids. The sequences with an RdRP
187 coding region were excluded, and the circularity of the sequences, as well as the
188 presence of an ORF encoding a tombusvirus-like capsid, were confirmed with Geneious
189 11.0.4 (Biomatters, Ltd).

190 **Annotation of crucivirus putative genes.**

191 The 461 cruciviral sequences were annotated and analyzed in Geneious 11.0.4.
192 Coding sequences (CDSs) were semi-automatically annotated from a custom database
193 (Supp. Table 3) of protein sequences of published cruciviruses and close homologs
194 obtained from GenBank, using Geneious 11.0.4's annotation function with a 25%
195 nucleotide similarity threshold. Annotated CDS were re-checked with GenBank
196 database using BLASTx to identify sequences similar to previously described
197 cruciviruses and putative relatives. Sequences containing in-frame stop codons were
198 checked for putative splicing sites (54), or translated using a ciliate genetic code only
199 when usage rendered a complete ORF with similarity to other putative crucivirus CDSs.
200 Predicted ORFs longer than 300 bases with no obvious homologs and no overlap with
201 CP or Rep-like ORFs were annotated as "putative ORFs".

202 **Putative Stem-loop annotation.**

203 Stem-loop structures that could serve as an origin of replication for circular
204 ssDNA viruses were identified and annotated using StemLoop-Finder (Pratt *et al.*,
205 unpublished, (55, 56)). The 461 cruciviral sequences were scanned for the presence of
206 conserved nonanucleotide motifs described for other CRESS-DNA viruses
207 (NANTANTAN, NAKWRTTAC, TAWWDHWAN, & TRAKATTRC) (12). The
208 integrated ViennaRNA 2.0 library was used to predict secondary structures of DNA
209 around the detected motif, including the surrounding 15-20 nucleotides on either side
210 (57, 58). Predicted structures with a stem longer than four base pairs and a loop
211 including seven or more bases were subjected to the default scoring system, which
212 increases the score by one point for each deviation from ideal stem lengths of 11 base
213 pairs and loop lengths of 11 nucleotides. A set of annotations for stem-loops and
214 nonanucleotides was created with StemLoop-Finder for those with a score of 15 or
215 below. Putative stem-loops were excluded from annotation when a separate stem-loop
216 was found with the same first base, but attained a greater score, as well as those that
217 appeared to have a nonanucleotide within four bases of its stem-loop structure's first or
218 last nucleotide.

219 **Conservation analysis and visualization**

220 *Pairwise identity matrices.* The pairwise identity (PI) between the protein sequence
221 from translated cruciviral genes was calculated with SDTv1.2 (59), with MAFFT
222 alignment option for CPs and S-domains, and MUSCLE alignment options for Reps.

223 *Sequence conservation annotation.* CP sequence conservation represented in Fig. 2A
224 was generated with Jalview v2.11.0 (60), and reflects the conservation of the
225 physicochemical properties for each column of the alignment (61).

226 *Sequence logos.* Sequence logos showing frequency of bases in nonanucleotides at the
227 origin of replication or residue in conserved Rep motifs were made using the weblogo
228 server (<http://weblogo.threeplusone.com/>; (62)).

229 *Structural representation of capsid conservation.* The 3D structure of CP was modeled
230 with Phyre² (63). The generated graphic was colored by sequence conservation with
231 Chimera v.1.13 (64), from the alignment of the 47 capsid sequences from each of the
232 CP-based clusters (Fig. 3B).

233 **Phylogenetic analyses.**

234 *Multiple sequence alignments.* CP sequences were aligned using MAFFT (65) in
235 Geneious 11.0.4, with a G-INS-i algorithm and BLOSUM 45 as exchange matrix, with
236 an open gap penalty of 1.53 and an offset value of 0.123, and manually curated. Rep
237 protein sequences were aligned using PSI-Coffee [<http://tcoffee.crg.cat/>; (66)]. Rep
238 alignments were manually inspected and corrected in Geneious 11.0.4, and trimmed
239 using TrimAI v1.3 with a *strict plus* setting (67). To produce individual alignments of
240 the endonuclease and helicase domains the full length trimmed alignments were split at
241 the Walker A motif (45).

242 *Phylogenetic trees.* Phylogenetic trees containing the entire dataset of cruciviral
243 sequences were built on Geneious using the FastTree plugin (68). For the analysis of
244 sequence subsets, trees were inferred with PhyML 3.0 web server [[http://www.atgc-
245 montpellier.fr/phymal/](http://www.atgc-montpellier.fr/phymal/); (69)], using an aLRT SH-like support (70). The substitution
246 model for each analysis was automatically selected by the program.

247 *Intergene and interdomain comparison.* Tanglegrams were made using Dendroscope
248 v3.5.10 (71) to compare the phylogenies between different genes or domains within the
249 same set of crucivirus genomes.

250 *Sequence similarity networks.* A total of 540 CP amino acid sequences, and 600 Rep
251 amino acid sequences were uploaded to EFI-EST web server for the calculation of PIs
252 [<https://efi.igb.illinois.edu/efi-est/>; (72)]. A specific alignment score cutoff was
253 established for each dataset analyzed, and xgmml files generated by EFI-EST were
254 visualized and edited in Cytoscape v3.7.2 (73).

255 **Accession numbers**

256 Provided in Supp. Table 1.

257 **RESULTS & DISCUSSION**

258 **Expansion of the crucivirus group.**

259 To broaden our understanding of the diversity and relationships of cruciviruses,
260 461 uncharacterized circular DNA sequences containing predicted CDSs with sequence
261 similarity to the CP of tombusviruses were compiled from metagenomic sequencing
262 data. The data came from published and unpublished metagenomic studies, carried out
263 in a wide variety of environments, from permafrost to temperate lakes, and on various
264 organisms from red algae to invertebrates (Metagenomes and their metadata are
265 provided in Supp. Table 2). The selected genomes are assumed to be complete and
266 circular based on the terminal redundancy identified in *de novo* assembled genomes.

267 The cruciviral sequences were named sequentially, beginning with the smallest
268 genome, which was named CruV-81 to account for the 80 crucivirus genomes reported
269 in prior literature (15, 19, 28–31, 20–27). The average GC content of the newly
270 described cruciviral sequences is $42.9 \pm 4.9\%$ (Fig. 1B) with genome lengths spanning
271 from 2,474 to 7,947 bases (Fig. 1A), some exceeding the size of described
272 bacilladnaviruses ($\leq 6,000$ nt (74)), the largest CRESS-DNA viruses known (12).

273 Of the 461 sequences that contain a CP ORF, 451 have putative coding regions
274 with sequence similarity to Rep of CRESS-DNA viruses (10). The CP and Rep ORFs
275 are encoded in a unisense orientation in 40% of the genomes and an ambisense
276 orientation in 58% of the genomes. The remaining ~2% correspond to ten CruCGEs
277 with no clear Rep CDS. Five of these CruCGEs contain a predicted origin of rolling-
278 circle replication (RCR) (Supp. Table 1), indicating that they are circular genomes that
279 undergo RCR characteristic of other CRESS-DNA virus genomes (16, 17).

280 One possible reason for the lack of a Rep ORF in certain sequences is that some
281 of these may be sub-genomic molecules or possible components of multipartite viruses
282 (75). Some CRESS-DNA viruses, such as geminiviruses and nanoviruses, have
283 multipartite genomes (76). Moreover, some ssRNA tombunodaviruses; including
284 *Plasmopara halstedii* virus A and *Schlerophthora macrospora* virus A –viruses that
285 contain the most similar capsid sequences to cruciviral capsids (15, 27)– also have
286 multipartite genomes (77). Unfortunately, no reliable method yet exists to match
287 different sequences belonging to the same multisegmented virus in metagenomes,

288 making identification of multipartite or segmented viruses from metagenomic data
289 challenging (76).

290 Stem-loop structures with conserved nonanucleotide motifs as putative origins
291 of replication were predicted and annotated in 277 cruciviral sequences with StemLoop-
292 Finder (Pratt *et al.*, unpublished). In some cases, more than one nonanucleotide motif
293 with similar scores were found for a single genome, resulting in more than one stem-
294 loop annotation. Of the annotated genomes, 223 contain a stem-loop with a
295 nonanucleotide with a NANTANTAN pattern, with the most common sequence being
296 the canonical circovirus motif TAGTATTAC, found in 64 of the genomes (Supp. Table
297 1; (78)). The majority of the 54 sequences that do not correspond to NANTANTAN
298 contain a TAWWDHWAN nonanucleotide motif, typical of genomoviruses (79). The
299 frequency of bases at each position in the nonanucleotide sequence is given in Fig. 1C,
300 and reflects similarity to motifs found in other CRESS-DNA viruses (10).

301 **Crucivirus capsid protein (CP)**

302 The CP of cruciviruses is predicted to have a single jelly-roll (SJR) architecture,
303 based on its homology to tombusvirus CPs for which 3D structures have been
304 determined [Fig. 2A; (80–82)]. The SJR conformation is found in CPs of both RNA and
305 DNA viruses (46). The SJR CP of tombusviruses and cruciviruses contains three
306 distinct domains: the RNA-binding or R-domain, the shell or S-domain, and the
307 protruding or P-domain (Fig. 2A). All 461 crucivirus CPs analyzed in this study contain
308 a complete S-domain. This domain contains a distinct jelly-roll fold and interacts with
309 the S-domain of other capsid subunits in the virion of related tombusviruses (48). The
310 S-domain has greater sequence conservation than the remaining regions of the CP (Fig.
311 2A), likely due to its functional importance in capsid structure. In tombusviruses, the S-
312 domain contains a calcium binding motif (DxDxxD), which was not identified in
313 previously described cruciviruses (83). However, we detected this Ca-binding motif in
314 68 CPs of the newly identified cruciviral sequences. These crucivirus sequences form a
315 distinct cluster, shown in red in Fig. 3B. The S-domain is flanked on the N-terminus by
316 the R-domain, which in cruciviruses appears variable in size (up to 320 amino acids
317 long), and appears to be truncated in some of the CP sequences (e.g. CruV-386 and
318 CruV-493). The R-domain is characterized by an abundance of basic residues at the N-

319 terminus, followed by a Gly-rich tract (Fig. 2A). The P-domain, on the C-terminal end
320 of the CP sequence, is generally the largest domain, with the exception of CruV-385,
321 where it appears to be truncated. The conservation of CP suggests a similar structure for
322 all cruciviruses. However, those cruciviruses with larger genomes may assemble their
323 capsids in a different arrangement to accommodate their genome. While the capsids of
324 tombusviruses have been shown to adopt a T=1 icosahedral conformation, rather than
325 the usual T=3, when the R-domain is partially or totally removed (82), we have not seen
326 a correlation between the length of CP domains and genome size in our dataset that
327 could be indicative of alternative capsid arrangements. Furthermore, no packaging
328 dynamics relating genome size and virion T-number arrangement have been determined
329 in CRESS-DNA viruses, although sub-genomic elements of geminiviruses can be
330 packaged in non-geminate capsids (84, 85).

331 Interestingly, CruV-420 contains not one tombusvirus-related CP, but two. A
332 recent compilation of CRESS-DNA viruses from animal metagenomes also contains
333 four genomes with two different CPs in their capsid (31). Whether these viruses use two
334 different CPs in their capsid (as some RNA viruses do), or whether these are
335 intermediates in the exchange of CP genes, as predicted from the gene capture
336 mechanism proposed by Stedman (2013) (18), is unclear. If the latter is true, CP gene
337 acquisition by CRESS-DNA viruses may be much more common than previously
338 thought.

339 **Crucivirus Rep**

340 The Reps of CRESS-DNA viruses typically contain an endonuclease domain
341 characterized by conserved motifs I, II and III, and a helicase domain with Walker A
342 and B motifs, motif C, and an Arg-finger [Fig. 2B; (12)]. The majority (85.9%) of the
343 crucivirus genomes described in this dataset contain all of the expected Rep motifs
344 (Supp. Table 4). However, five genomes (CruCGE-110, CruCGE-296, CruCGE-436,
345 CruCGE-471 and CruCGE-533) with overall sequence homology to other Reps (35.8,
346 32.7, 49.7, 60.2 and 57.2 % PI with other putative Reps in the databases, respectively),
347 lack any detectable conserved motifs within their sequence. Thus, these sequences are
348 considered CP-encoding cruci-like circular genetic elements (CruCGEs).

349 The endonuclease catalytic domain of Rep (motif II), including HUH, was
350 identified in 441 of the genomes of which 95.2% had an alternative HUH, with the most
351 common arrangement being HUQ (70.0%), also found in circoviruses and nanoviruses
352 [(10, 25, 39); Fig. 2B]. 26.2% of the crucivirus motif II deviate from the HUH motif by
353 additionally replacing the second hydrophobic residue (U) with a polar amino acid (Fig.
354 2B; supp. Table 4), with 53 of Reps with the sequence HYQ (12.0%), also found in
355 smacoviruses (10, 23, 45).

356 We identified thirteen putative Reps in these crucivirus genomes that lack all
357 four motifs typically found in S3H helicases (e.g. CruV-166, CruV-202, CruV-499;
358 Supp. Table 4). Recent work has shown that the deletion of individual conserved motifs
359 in the helicase domain of the Rep protein of beak and feather disease virus does not
360 abolish ATPase and GTPase activity (86). The absence of all four motifs may prevent
361 these putative Reps from performing helicase and ATPase activity using previously
362 characterized mechanisms. However, it is possible that crucivirus Reps that lack these
363 motifs are still capable of ATP hydrolysis and associated helicase activity.
364 Alternatively, these activities may be provided by host factors (87), or by a viral
365 replication-enhancer protein – as is the case with the AC3 protein of begomoviruses
366 (88).

367 We identified 36 crucivirus genomes whose putative *rep* genes contain in-frame
368 stop codons or the HUH and SF3 helicase are in different frames, suggesting that their
369 transcripts may require intron splicing prior to translation. Acceptor and donor splicing
370 sites identical to those found in maize streak virus (54) were found in all these
371 sequences, and the putatively spliced Reps annotated accordingly. In five of the 36
372 spliced Reps, we were unable to detect any of the four conserved motifs associated with
373 helicase/ATPase activity, which are encoded in the predicted second exon in most cases.
374 CruV-513 and CruV-518 also contain predicted splicing sites in their CP gene.

375 No GRS motifs –which have been identified as necessary for geminivirus
376 replication (89), and have also been found in genomoviruses (90)– were detected in
377 Reps in our dataset. We were unable to detect any conserved Rep motifs present in
378 cruciviruses that are absent in other CRESS-DNA viruses. Given the conservation of
379 Rep motifs in these newly-described cruciviruses, we expect most to be active in RCR.

380 **Crucivirus CPs share higher genetic identity than their Rep proteins**

381 To assess the diversity in the proteins of cruciviruses, the percentage pairwise
382 identity (% PI) between the protein sequences was calculated for CP and Rep using
383 SDTv1.2 (Fig. 3). The average % PI for CP was found to be 33.1 ± 4.9 % PI (Figs. 3A
384 and 3D), likely due to the high levels of conservation found in the S-domain (40.5 ± 8.4
385 % PI; Figs. 3B and 3D), while the average % PI for Rep is quite low at 24.7% (± 5.6
386 SD; Figs. 3C and 3D). The high variation of the Rep protein sequence relative to CP in
387 cruciviruses correlates with a previous observation on a smaller dataset (20).

388 To compare cruciviruses to other viral groups with homologous proteins,
389 sequence similarity networks were built for CP and Rep (Fig. 4). For the CP, related
390 protein sequences from tombusviruses and unclassified RNA viruses were included.
391 The virus sequences were connected when the similarity between their protein sequence
392 had an e-value $< 1e-20$, sufficient to connect all cruciviruses and tombusviruses, with
393 the exception of CruV-523 (Fig. 4A). However, using BLASTp, CruV-523 showed
394 similarity to other RNA viruses with an e-value $< 1e-9$, which were not included in the
395 analysis. The CP sequence similarity network analysis demonstrates the apparent
396 homology of the CPs in our dataset with the CP of RNA viruses; specifically to
397 unclassified RNA viruses that have RdRPs similar to either tombusviruses –also
398 described as tombus-like viruses (77, 91, 92)– or to nodaviruses. The latter RNA viruses
399 are proposed to belong to a chimeric group of viruses named tombunodaviruses (93).

400 For sequence similarity network analysis of Rep, sequences from CRESS-DNA
401 viruses belonging to the families *Circoviridae*, *Nanoviridae*, *Alphasatellitidae*,
402 *Geminiviridae*, *Genomoviridae*, *Smacoviridae* and *Bacilladnaviridae* were used (Fig.
403 4B). Due to the heterogeneity of Rep (Fig. 3C), the score cutoff for the network was
404 relaxed to an e-value $< 1e-10$; nonetheless, ten divergent sequences lacked sufficient
405 similarity to form connections within the network. While the Rep of the different viral
406 families clustered in specific regions of the network, the similarity of cruciviral Reps
407 spans the diversity of all CRESS-DNA viruses, and blurs the borders between them.
408 Though there are cruciviruses that appear to be closely related to geminiviruses and
409 genomoviruses, these connections are less common than with other classified CRESS-
410 DNA families (Fig. 4B). While still highly divergent from each other, the conserved

411 motifs in the Rep still share the most sequence similarity with CRESS-DNA viruses
412 (Fig. 2B).

413 The broad sequence space distribution of cruciviral Rep sequences has been
414 proposed to reflect multiple Rep acquisition events through recombination with viruses
415 from different CRESS-DNA viral families (20). However, the apparent larger diversity
416 of cruciviral Reps relative to classified CRESS-DNA viruses can be due to the method
417 of study, as most classified CRESS-DNA viruses have been discovered from infected
418 organisms and are grouped mainly based on Rep similarity (1). By contrast, here
419 crucivirus sequences are selected according to the presence of a tombusvirus-like CP.
420 Moreover, the Rep of cruciviruses could be subject to higher substitution rates than CP
421 (26). It is possible that sequence divergence in CP is more limited than in the Rep due to
422 structural constraints.

423 **Horizontal gene transfer among cruciviruses.**

424 To gain insight into the evolutionary history of cruciviruses, we carried out
425 phylogenetic analyses of their CPs and Reps. Due to the high sequence diversity in the
426 dataset, two smaller subsets of sequences were analyzed:

427 i) *CP-based clusters*. Clusters with more than six non-identical CP sequences whose S-
428 domains share a % PI greater than 70% were identified from Fig. 3B. This resulted in
429 the identification of seven clusters, and a more divergent, yet clearly distinct, cluster
430 was included (pink in Fig. 3B). A total of 47 genomes from the eight different clusters
431 were selected for sequence comparison. The protein sequences of CP and Rep were
432 extracted, aligned, and their phylogenies inferred and analyzed using tanglegrams (Fig.
433 5A). The CP phylogeny shows that the eight CP-based clusters form separate clades
434 (Fig. 5A). On the other hand, the phylogeny of Rep shows a different pattern of
435 relatedness between those genomes (Fig. 5A). This suggests different evolutionary
436 histories for the CP and Rep proteins, which could be due to recombination events
437 between cruciviruses, as previously proposed with smaller datasets (20, 21).

438 ii) *Rep-based clusters*. To account for the possible bias introduced by selecting genomes
439 from CP cluster groups and to increase the resolution in the phylogeny of the Rep
440 sequences, clusters with more than six Rep sequences sharing PI > 45 and < 98% were

441 identified. A total of 53 genomes from six clusters (Fig. 3C) were selected, and their CP
442 and Rep protein sequences analyzed. The phylogeny of Reps shows distinct clades
443 between the sequences from different clusters (Fig. 5B). When the phylogeny of Rep
444 was compared to that of their corresponding CPs, we observed the presence of groups of
445 cruciviruses that clade with each other in both the Rep and the CP. Discrepancies in
446 topology between Rep and CP were observed as well, particularly in the CP clade
447 marked with an asterisk in Fig. 5B. This clade corresponds to the highly-homogeneous
448 red CP-based cluster shown in Fig. 3B, and suggests that gene transfer is more common
449 in cruciviruses with a more similar CP, likely infecting the same type of organism. On
450 the other hand, the presence of cruciviral groups with no trace of genetic exchange may
451 indicate that lineages within the cruciviral group may have undergone speciation in the
452 course of evolution.

453 To investigate possible exchanges of individual Rep domains among
454 cruciviruses, the Rep alignments of the analyses of the CP-based and Rep-based clusters
455 were split at the beginning of the Walker A motif to separate endonuclease and helicase
456 domains. From the analysis of the CP-based clusters, we observed incongruence in the
457 phylogenies between endonuclease and helicase domains (Fig. 6A), suggesting
458 recombination within crucivirus Reps, as has been previously hypothesized with a much
459 smaller dataset (21). This incongruency is not observed in the analyzed Rep-based
460 clusters (Fig. 6B). This is likely due to the higher similarity between Reps in this subset
461 of sequences, biased by the clustering based on Rep. We do observe different topologies
462 between the trees, which may be a consequence of different evolutionary constraints to
463 which the endonuclease and helicase domains are subject. The detection of CP/Rep
464 exchange and not of individual Rep domains in Rep-based clusters suggests that the rate
465 of intergenic recombination is higher than intragenic recombination in cruciviruses.

466 **Members of the SAR supergroup are potential crucivirus hosts**

467 While no crucivirus host has been identified to date, the architecture of the Rep
468 protein found in most cruciviruses, as well as the presence of introns in some of the
469 genomes, suggests a eukaryotic host. The fusion of an endonuclease domain to a S3H
470 helicase domain is observed in other CRESS-DNA viruses which are known to infect
471 eukaryotes (38). This is distinct from Reps found in prokaryote-infecting CRESS-DNA

472 viruses –which lack a fused S3H helicase domains (94)– and other related HUH
473 endonucleases involved in plasmid RCR and HUH transposases (38). Additionally, the
474 CP of cruciviruses, a suggested determinant of tropism (95, 96), is homologous to the
475 capsid of RNA viruses known to infect eukaryotes. The RNA viruses with a known host
476 with capsids most similar to cruciviral capsids (tombunodaviruses) infect oomycetes, a
477 group of filamentous eukaryotic stramenopiles (77).

478 Cruciviruses have been found as contaminants of spin columns made of
479 diatomaceous silica (21), in aquatic metagenomes enriched with unicellular algae (20),
480 in the metagenome of *Astrammina rara* –a foraminiferan protist part of the rhizaria–
481 (20), and associated with epibionts of isopods, mainly comprised of apicomplexans and
482 ciliates, both belonging to the alveolates (26). These pieces of evidence point toward the
483 stramenopiles/alveolates/rhizaria (SAR) supergroup as a candidate taxon to contain
484 potential crucivirus hosts (97). No host prediction can be articulated from our sequence
485 data. However, at least five of the crucivirus genomes only render complete translated
486 CP and Rep sequences when using a relaxed genetic code. Such alternative genetic
487 codes have been detected in ciliates, in which the hypothetical termination codons UAA
488 and UAG encode for a glutamine (98). The usage of an alternative genetic code seems
489 evident in CruV-502 –found in the metagenome from seawater collected above diseased
490 coral colonies (99)– that uses a UAA codon for a glutamine of the S-domain conserved
491 in 33.5% of the sequences. While the data accumulated suggest unicellular eukaryotes
492 and SAR members as crucivirus-associated organisms, the host of cruciviruses remains
493 elusive, and further investigations are necessary.

494 ***Classification of cruciviruses***

495 Cruciviruses have circular genomes that encode a Rep protein probably involved
496 in RCR. The single-stranded nature of packaged crucivirus genomes has not been
497 demonstrated experimentally; however, the overall genomic structure and sequence
498 similarity underpins the placement of cruciviruses within the CRESS-DNA viruses.

499 The classification of the CRESS-DNA viruses is primarily based upon the
500 phylogeny of the Rep proteins, although commonalities in CP and genome organization
501 are also considered (13). This taxonomic criteria is challenging in cruciviruses, whose

502 Rep proteins are highly diverse and apparently paralogous. Whether the use of proteins
503 involved in replication for virus classification should be preferred over structural
504 proteins has been previously questioned (100).

505 The capsid of cruciviruses, as well as the capsid of other CRESS-DNA virus
506 families like circoviruses, geminiviruses and bacilladnaviruses, possess the single-jelly
507 roll architecture (46). However, there is no obvious sequence similarity between the CP
508 of cruciviruses and that of classified CRESS-DNA viruses. The crucivirus CP –
509 homologous to the capsid of tombusviruses– is an orthologous trait within the CRESS-
510 DNA viruses. Hence, CP constitutes a synapomorphic character that demarcate this
511 group of viruses from the rest of the CRESS-DNA viral families. Thus, the
512 classification of cruciviruses is challenging.

513 CONCLUDING REMARKS

514 Cruciviruses are a growing group of CRESS-DNA viruses that encode CPs that
515 are homologous to those encoded by tombusviruses. Over 500 crucivirus genomes have
516 been recovered from various environments across the globe. These genomes vary in
517 size, sequence and genome organization. While crucivirus CPs are relatively
518 homogeneous, the Reps are relatively diverse amongst the cruciviruses, spanning the
519 diversity of all classified CRESS-DNA viruses. It has been hypothesized that
520 cruciviruses emerged from the recombination between a CRESS-DNA virus and a
521 tombus-like RNA virus (15, 18). Furthermore, cruciviruses seem to have recombined
522 with each other to exchange functional modules between them, and probably with other
523 viral groups, which blurs their evolutionary history. Cruciviruses show evidence of
524 genetic transfer, not just between viruses with similar genomic properties, but also
525 between disparate groups of viruses such as CRESS-DNA and RNA viruses.

526 ACKNOWLEDGEMENTS

527 This work was supported by the NASA Exobiology Program, grant
528 80NSSC17K0301 (I. dl H., G. K., E. T., A. P. and K. S.), the NIH BUILD EXITO
529 Program (A. M.), BUILD EXITO was supported by grants from the National Institutes
530 of Health: UL1GM118964; RL5GM118963; TL4GM118965, and the Portland State

531 University Ronald E. McNair Scholars Program (E. T.), supported by grants from the
532 U.S. Department of Education and Portland State University. The Antarctic field work
533 was supported by the US National Science Foundation (NSF) under grant ANT-
534 0944411, with logistics supplied by the US Antarctic Program. The fresh water work in
535 New Zealand was supported by a grant (UC-E6007) from the American New Zealand
536 Association (USA) awarded to P. Z-R., C. G., J. S. H. and A. V. The green lipped
537 mussel work was supported by a grant from the Brian Mason Scientific & Technical
538 Trust of New Zealand awarded to S.G. and A.V. EU-s Horizon 2020 Framework
539 Program for Research and Innovation ('Virus-X', project no. 685778) supported F. E.

540

BIBLIOGRAPHY

541

1. Simmonds P, Adams MJ, Benk M, Breitbart M, Brister JR, Carstens EB, Davison AJ, Delwart E, Gorbalenya AE, Harrach B, Hull R, King AMQ, Koonin E V., Krupovic M, Kuhn JH, Lefkowitz EJ, Nibert ML, Orton R, Roossinck MJ, Sabanadzovic S, Sullivan MB, Suttle CA, Tesh RB, Van Der Vlugt RA, Varsani A, Zerbini FM. 2017. Consensus statement: Virus taxonomy in the age of metagenomics. *Nat Rev Microbiol* 15:161–168.
2. Chow C-ET, Suttle CA. 2015. Biogeography of Viruses in the Sea. *Annu Rev Virol* 2:41–66.
3. Koonin E V., Dolja V V. 2013. A virocentric perspective on the evolution of life. *Curr Opin Virol* 3:546–557.
4. Koonin E V., Krupovic M. 2018. The depths of virus exaptation. *Curr Opin Virol* 31:1–8.
5. Berliner AJ, Mochizuki T, Stedman KM. 2018. Astrovirology: Viruses at Large in the Universe. *Astrobiology* 18:207–223.
6. Domingo E, Sheldon J, Perales C. 2012. Viral Quasispecies Evolution. *Microbiol Mol Biol Rev* 76:159–216.
7. Baltimore D. 1971. Expression of animal virus genomes. *Bacteriol Rev* 35:235–241.
8. Koonin E V., Senkevich TG, Dolja V V. 2006. The ancient virus world and evolution of cells. *Biol Direct* 1.
9. Krupovic M, Ravantti JJ, Bamford DH. 2009. Geminiviruses: A tale of a plasmid becoming a virus. *BMC Evol Biol* 9:1–11.
10. Kazlauskas D, Varsani A, Koonin E V., Krupovic M. 2019. Multiple origins of prokaryotic and eukaryotic single-stranded DNA viruses from bacterial and archaeal plasmids. *Nat Commun* 10:1–12.
11. Krupovic M. 2012. Recombination between RNA viruses and plasmids might have played a central role in the origin and evolution of small DNA viruses. *BioEssays* 34:867–870.
12. Zhao L, Rosario K, Breitbart M, Duffy S. 2019. Eukaryotic Circular Rep-Encoding Single-Stranded DNA (CRESS DNA) Viruses: Ubiquitous Viruses With Small Genomes and a Diverse Host Range. *Adv Virus Res*, 1st ed. 103:71–133.
13. Rosario K, Duffy S, Breitbart M. 2012. A field guide to eukaryotic circular single-stranded DNA viruses: Insights gained from metagenomics. *Arch Virol* 157:1851–1871.
14. Cheung AK. 2015. Specific functions of the Rep and Rep' proteins of porcine circovirus during copy-release and rolling-circle DNA replication. *Virology* 481:43–50.
15. Diemer GS, Stedman KM. 2012. A novel virus genome discovered in an extreme environment suggests recombination between unrelated groups of RNA and DNA viruses. *Biol Direct* 7:13.
16. Cheung AK. 2012. Porcine circovirus: Transcription and DNA replication. *Virus Res* 164:46–53.
17. LAUFS J. 1995. Geminivirus replication: Genetic and biochemical characterization of rep protein function, a review. *Biochimie* 77:765–773.
18. Stedman K. 2013. Mechanisms for RNA capture by ssDNA viruses: Grand theft RNA. *J Mol Evol* 76:359–364.

578 19. Rosario K, Dayaram A, Marinov M, Ware J, Kraberger S, Stainton D, Breitbart M, Varsani A.
579 2012. Diverse circular ssDNA viruses discovered in dragonflies (Odonata: Epiprocta). *J Gen*
580 *Virol* 93:2668–2681.

581 20. Roux S, Enault F, Bronner G, Vaulot D, Forterre P, Krupovic M. 2013. Chimeric viruses blur the
582 borders between the major groups of eukaryotic single-stranded DNA viruses. *Nat Commun*
583 4:2700.

584 21. Krupovic M, Zhi N, Li J, Hu G, Koonin E V., Wong S, Shevchenko S, Zhao K, Young NS. 2015.
585 Multiple layers of chimerism in a single-stranded DNA virus discovered by deep sequencing.
586 *Genome Biol Evol* 7:993–1001.

587 22. Hewson I, Ng G, Li WF, LaBarre BA, Aguirre I, Barbosa JG, Breitbart M, Greco AW, Kearns
588 CM, Looi A, Schaffner LR, Thompson PD, Hairston NG. 2013. Metagenomic identification,
589 seasonal dynamics, and potential transmission mechanisms of a *Daphnia*-associated single-
590 stranded DNA virus in two temperate lakes. *Limnol Oceanogr* 58:1605–1620.

591 23. Steel O, Kraberger S, Sikorski A, Young LM, Catchpole RJ, Stevens AJ, Ladley JJ, Coray DS,
592 Stainton D, Dayaram A, Julian L, van Bysterveldt K, Varsani A. 2016. Circular replication-
593 associated protein encoding DNA viruses identified in the faecal matter of various animals in
594 New Zealand. *Infect Genet Evol* 43:151–164.

595 24. McDaniel LD, Rosario K, Breitbart M, Paul JH. 2014. Comparative metagenomics: natural
596 populations of induced prophages demonstrate highly unique, lower diversity viral sequences.
597 *Environ Microbiol* 16:570–585.

598 25. Dayaram A, Galatowitsch ML, Argüello-Astorga GR, van Bysterveldt K, Kraberger S, Stainton
599 D, Harding JS, Roumagnac P, Martin DP, Lefevre P, Varsani A. 2016. Diverse circular
600 replication-associated protein encoding viruses circulating in invertebrates within a lake
601 ecosystem. *Infect Genet Evol* 39:304–316.

602 26. Bistolas K, Besemer R, Rudstam L, Hewson I. 2017. Distribution and Inferred Evolutionary
603 Characteristics of a Chimeric ssDNA Virus Associated with Intertidal Marine Isopods. *Viruses*
604 9:361.

605 27. Quaiser A, Krupovic M, Dufresne A, Francez A-J, Roux S. 2016. Diversity and comparative
606 genomics of chimeric viruses in Sphagnum- dominated peatlands. *Virus Evol* 2:vew025.

607 28. Salmier A, Tirera S, de Thoisy B, Franc A, Darcissac E, Donato D, Bouchier C, Lacoste V,
608 Lavergne A. 2017. Virome analysis of two sympatric bat species (*Desmodus rotundus* and
609 *Molossus molossus*) in French Guiana. *PLoS One* 12:e0186943.

610 29. de la Higuera I, Torrance EL, Pratt AA, Kasun GW, Maluenda A, Stedman KM. 2019. Genome
611 Sequences of Three Cruciviruses Found in the Willamette Valley (Oregon). *Microbiol Resour*
612 *Announc* 8.

613 30. Kraberger S, Argüello-Astorga GR, Greenfield LG, Galilee C, Law D, Martin DP, Varsani A.
614 2015. Characterisation of a diverse range of circular replication-associated protein encoding DNA
615 viruses recovered from a sewage treatment oxidation pond. *Infect Genet Evol* 31:73–86.

616 31. Tisza MJ, Pastrana D V, Welch NL, Stewart B, Peretti A, Starrett GJ, Pang Y-YS, Krishnamurthy
617 SR, Pesavento PA, McDermott DH, Murphy PM, Whited JL, Miller B, Brenchley J, Rosshart SP,
618 Rehermann B, Doorbar J, Ta’ala BA, Pletnikova O, Troncoso JC, Resnick SM, Bolduc B,
619 Sullivan MB, Varsani A, Segall AM, Buck CB. 2020. Discovery of several thousand highly
620 diverse circular DNA viruses. *Elife* 9:555375.

621 32. Brown DR, Schmidt-Glenewinkel T, Reinberg D, Hurwitz J. 1983. DNA sequences which
622 support activities of the bacteriophage phiX174 gene A protein.

623 33. Steinfeldt T, Finsterbusch T, Mankertz A. 2006. Demonstration of Nicking/Joining Activity at the
624 Origin of DNA Replication Associated with the Rep and Rep' Proteins of Porcine Circovirus
625 Type 1. *J Virol* 80:6225–6234.

626 34. Gassmann M, Focher F, Buhk HJ, Ferrari E, Spadari S, Hübscher U. 1988. Replication of single-
627 stranded porcine circovirus DNA by DNA polymerases α and δ . *BBA - Gene Struct Expr*.

628 35. Roth MJ, Brown DR, Hurwitz J. 1984. Analysis of Bacteriophage phi174 Gene A Protein-
629 mediated Termination and Reinitiation of 6X DNA Synthesis 11. Structural characterization of
630 the covalent 4X A protein-DNA complex. *J. Biol. Chern.*

631 36. Cheung AK. 2007. A stem-loop structure, sequence non-specific, at the origin of DNA replication
632 of porcine circovirus is essential for termination but not for initiation of rolling-circle DNA
633 replication. *Virology* 363:229–235.

634 37. Stenger DC, Revington GN, Stevenson MC, Bisaro DM. 1991. Replicational release of
635 geminivirus genomes from tandemly repeated copies: Evidence for rolling-circle replication of a
636 plant viral DNA. *Proc Natl Acad Sci U S A*.

637 38. Chandler M, de la Cruz F, Dyda F, Hickman AB, Moncalian G, Ton-Hoang B. 2013. Breaking
638 and joining single-stranded DNA: the HUH endonuclease superfamily. *Nat Rev Microbiol*
639 11:525–538.

640 39. Brown DR, Schmidt-Glenewinkel T, Reinberg D, Hurwitz J. 1983. DNA sequences which
641 support activities of the bacteriophage phiX174 gene A protein 258:8402–8412.

642 40. Ilyina T V., Koonin E V. 1992. Conserved sequence motifs in the initiator proteins for rolling
643 circle DNA replication encoded by diverse replicons from eubacteria, eucaryotes and
644 archaebacteria. *Nucleic Acids Res* 20:3279–3285.

645 41. Koonin E V, Ilyina T V. 1993. Computer-assisted dissection of rolling circle DNA replication.
646 *BioSystems* 30:241–268.

647 42. Londoño A, Riego-Ruiz L, Argüello-Astorga GR. 2010. DNA-binding specificity determinants of
648 replication proteins encoded by eukaryotic ssDNA viruses are adjacent to widely separated RCR
649 conserved motifs. *Arch Virol* 155:1033–1046.

650 43. Gorbalenya AE, Koonin E V. 1993. Helicases: amino acid sequence comparisons and structure-
651 function relationships. *Curr Opin Struct Biol* 3:419–429.

652 44. Clerot D, Bernardi F. 2006. DNA Helicase Activity Is Associated with the Replication Initiator
653 Protein Rep of Tomato Yellow Leaf Curl Geminivirus. *J Virol* 80:11322–11330.

654 45. Kazlauskas D, Varsani A, Krupovic M. 2018. Pervasive chimerism in the replication-associated
655 proteins of uncultured single-stranded DNA viruses. *Viruses* 10:1–11.

656 46. Krupovic M, Koonin E V. 2017. Multiple origins of viral capsid proteins from cellular ancestors.
657 *Proc Natl Acad Sci U S A* 114:E2401–E2410.

658 47. Hopper P, Harrison SC, Sauer RT. 1984. Structure of tomato bushy stunt virus. V. Coat protein
659 sequence determination and its structural implications. *J Mol Biol* 177:701–713.

660 48. Sherman MB, Guenther R, Reade R, Rochon D, Sit T, Smith TJ. 2019. Near-Atomic-Resolution
661 Cryo-Electron Microscopy Structures of Cucumber Leaf Spot Virus and Red Clover Necrotic
662 Mosaic Virus: Evolutionary Divergence at the Icosahedral Three-Fold Axes. *J Virol* 94.

663 49. Alam SB, Reade R, Theilmann J, Rochon DA. 2017. Evidence for the role of basic amino acids in
664 the coat protein arm region of Cucumber necrosis virus in particle assembly and selective
665 encapsidation of viral RNA. *Virology* 512:83–94.

666 50. Park SH, Sit TL, Kim KH, Lommel SA. 2013. The red clover necrotic mosaic virus capsid
667 protein N-terminal amino acids possess specific RNA binding activity and are required for stable
668 virion assembly. *Virus Res* 176:107–118.

669 51. Ohki T, Akita F, Mochizuki T, Kanda A, Sasaya T, Tsuda S. 2010. The protruding domain of the
670 coat protein of Melon necrotic spot virus is involved in compatibility with and transmission by
671 the fungal vector *Olpidium bornovanus*. *Virology* 402:129–134.

672 52. Llauró A, Coppari E, Imperatori F, Bizzarri AR, Castón JR, Santi L, Cannistraro S, De Pablo PJ.
673 2015. Calcium Ions Modulate the Mechanics of Tomato Bushy Stunt Virus. *Biophys J* 109:390–
674 397.

675 53. Paez-Espino D, Chen I-MA, Palaniappan K, Ratner A, Chu K, Szeto E, Pillay M, Huang J,
676 Markowitz VM, Nielsen T, Huntemann M, K. Reddy TB, Pavlopoulos GA, Sullivan MB,
677 Campbell BJ, Chen F, McMahon K, Hallam SJ, Denef V, Cavicchioli R, Caffrey SM, Streit WR,
678 Webster J, Handley KM, Salekdeh GH, Tsesmetzis N, Setubal JC, Pope PB, Liu W-T, Rivers AR,
679 Ivanova NN, Kyrpides NC. 2017. IMG/VR: a database of cultured and uncultured DNA Viruses
680 and retroviruses. *Nucleic Acids Res* 45:D457–D465.

681 54. Wright EA, Heckel T, Groenendijk J, Davies JW, Boulton MI. 1997. Splicing features in maize
682 streak virus virion- and complementary-sense gene expression. *Plant J* 12:1285–1297.

683 55. Steinfeldt T, Finsterbusch T, Mankertz A. 2006. Demonstration of Nicking/Joining Activity at the
684 Origin of DNA Replication Associated with the Rep and Rep' Proteins of Porcine Circovirus
685 Type 1. *J Virol* 80:6225–6234.

686 56. Hafner GJ, Dale JL, Harding RM, Wolter LC, Stafford MR. 1997. Nicking and joining activity of
687 banana bunchy top virus replication protein in vitro. *J Gen Virol* 78:1795–1799.

688 57. Lorenz R, Bernhart SH, Höner zu Siederdissen C, Tafer H, Flamm C, Stadler PF, Hofacker IL.
689 2011. ViennaRNA Package 2.0. *Algorithms Mol Biol* 6:26.

690 58. Mathews DH, Sabina J, Zuker M, Turner DH. 1999. Expanded sequence dependence of
691 thermodynamic parameters improves prediction of RNA secondary structure. *J Mol Biol*
692 288:911–940.

693 59. Muhire BM, Varsani A, Martin DP. 2014. SDT: A Virus Classification Tool Based on Pairwise
694 Sequence Alignment and Identity Calculation. *PLoS One* 9:e108277.

695 60. Waterhouse AM, Procter JB, Martin DMA, Clamp M, Barton GJ. 2009. Jalview Version 2-A
696 multiple sequence alignment editor and analysis workbench. *Bioinformatics* 25:1189–1191.

697 61. Livingstone CD, Barton GJ. 1993. Protein sequence alignments: A strategy for the hierarchical
698 analysis of residue conservation. *Bioinformatics*.

699 62. Crooks GE, Hon G, Chandonia JM, Brenner SE. 2004. WebLogo: A sequence logo generator.
700 *Genome Res*.

701 63. Kelley LA, Mezulis S, Yates CM, Wass MN, Sternberg MJE. 2015. The Phyre2 web portal for
702 protein modeling, prediction and analysis. *Nat Protoc* 10:845–858.

703 64. Pettersen EF, Goddard TD, Huang CC, Couch GS, Greenblatt DM, Meng EC, Ferrin TE. 2004.
704 UCSF Chimera - A visualization system for exploratory research and analysis. *J Comput Chem*
705 25:1605–1612.

706 65. Katoh K, Standley DM. 2013. MAFFT Multiple Sequence Alignment Software Version 7:
707 Improvements in Performance and Usability. *Mol Biol Evol* 30:772–780.

708 66. Floden EW, Tommaso PD, Chatzou M, Magis C, Notredame C, Chang J-M. 2016. PSI/TM-
709 Coffee: a web server for fast and accurate multiple sequence alignments of regular and
710 transmembrane proteins using homology extension on reduced databases. *Nucleic Acids Res*
711 44:W339–W343.

712 67. Capella-Gutiérrez S, Silla-Martínez JM, Gabaldón T. 2009. trimAl: A tool for automated
713 alignment trimming in large-scale phylogenetic analyses. *Bioinformatics*.

714 68. Price MN, Dehal PS, Arkin AP. 2009. Fasttree: Computing large minimum evolution trees with
715 profiles instead of a distance matrix. *Mol Biol Evol* 26:1641–1650.

716 69. Guindon S, Dufayard JF, Lefort V, Anisimova M, Hordijk W, Gascuel O. 2010. New algorithms
717 and methods to estimate maximum-likelihood phylogenies: Assessing the performance of PhyML
718 3.0. *Syst Biol* 59:307–321.

719 70. Anisimova M, Gascuel O. 2006. Approximate Likelihood-Ratio Test for Branches: A Fast,
720 Accurate, and Powerful Alternative. *Syst Biol* 55:539–552.

721 71. Huson DH, Scornavacca C. 2012. Dendroscope 3: An interactive tool for rooted phylogenetic
722 trees and networks. *Syst Biol*.

723 72. Zallot R, Oberg N, Gerlt JA. 2019. The EFI Web Resource for Genomic Enzymology Web Tools:
724 Leveraging Protein, Genome, and Metagenome Databases to Discover Novel Enzymes and
725 Metabolic Pathways. *Biochemistry* acs.biochem.9b00735.

726 73. Shannon P, Markiel A, Ozier O, Baliga NS, Wang JT, Ramage D, Amin N, Schwikowski B,
727 Ideker T. 2003. Cytoscape: A software Environment for integrated models of biomolecular
728 interaction networks. *Genome Res* 13:2498–2504.

729 74. Kazlauskas D, Dayaram A, Kraberger S, Goldstien S, Varsani A, Krupovic M. 2017.
730 Evolutionary history of ssDNA bacilladnaviruses features horizontal acquisition of the capsid
731 gene from ssRNA nodaviruses. *Virology* 504:114–121.

732 75. Sicard A, Michalakis Y, Gutiérrez S, Blanc S. 2016. The Strange Lifestyle of Multipartite
733 Viruses. *PLoS Pathog* 12:1–19.

734 76. Varsani A, Lefevre P, Roumagnac P, Martin D. 2018. Notes on recombination and reassortment
735 in multipartite/segmented viruses. *Curr Opin Virol* 33:156–166.

736 77. Grasse W, Spring O. 2017. ssRNA viruses from biotrophic Oomycetes form a new phylogenetic
737 group between Nodaviridae and Tombusviridae. *Arch Virol* 162:1319–1324.

738 78. Rosario K, Mettel KA, Benner BE, Johnson R, Scott C, Yusseff-Vanegas SZ, Baker CCM,
739 Cassill DL, Storer C, Varsani A, Breitbart M. 2018. Virus discovery in all three major lineages of
740 terrestrial arthropods highlights the diversity of single-stranded DNA viruses associated with
741 invertebrates. *PeerJ* 6:e5761.

742 79. Varsani A, Krupovic M. 2017. Sequence-based taxonomic framework for the classification of
743 uncultured single-stranded DNA viruses of the family Genomoviridae. *Virus Evol* 3.

744 80. Harrison SC, Olson AJ, Schutt CE, Winkler FK, Bricogne G. 1978. Tomato bushy stunt virus at
745 2.9 Å resolution. *Nature* 276:368–373.

746 81. Chelvanayagam G, Heringa J, Argos P. 1992. Anatomy and Evolution of Proteins Displaying the
747 Viral Capsid Jellyroll Topology. *J Mol Biol* 228:220–242.

748 82. Katpally U, Kakani K, Reade R, Dryden K, Rochon D, Smith TJ. 2007. Structures of T=1 and
749 T=3 Particles of Cucumber Necrosis Virus: Evidence of Internal Scaffolding. *J Mol Biol*
750 365:502–512.

751 83. Campbell JW, Clifton IJ, Greenhough TJ, Hajdu J, Harrison SC, Liddington RC, Shrive AK.
752 1990. Calcium binding sites in tomato bushy stunt virus visualized by laue crystallography. *J Mol*
753 *Biol* 214:627–632.

754 84. Casado CG, Javier Ortiz G, Padron E, Bean SJ, McKenna R, Agbandje-McKenna M, Boulton MI.
755 2004. Isolation and characterization of subgenomic DNAs encapsidated in “single” T = 1
756 isometric particles of Maize streak virus. *Virology* 323:164–171.

757 85. Bennett A, Rodriguez D, Lister S, Boulton M, McKenna R, Agbandje-McKenna M. 2018.
758 Assembly and disassembly intermediates of maize streak geminivirus. *Virology* 525:224–236.

759 86. Chen JK, Hsiao C, Wu JS, Lin SY, Wang CY. 2019. Characterization of the endonuclease
760 activity of the replication-associated protein of beak and feather disease virus. *Arch Virol*
761 164:2091–2106.

762 87. Rizvi I, Choudhury NR, Tuteja N. 2015. Insights into the functional characteristics of geminivirus
763 rolling-circle replication initiator protein and its interaction with host factors affecting viral DNA
764 replication. *Arch Virol* 160:375–387.

765 88. Pasumarty KK, Choudhury NR, Mukherjee SK. 2010. Tomato leaf curl Kerala virus
766 (ToLCKeV) AC3 protein forms a higher order oligomer and enhances ATPase activity of
767 replication initiator protein (Rep/AC1). *Virol J* 7:128.

768 89. Nash TE, Dallas MB, Reyes MI, Buhrman GK, Ascencio-Ibanez JT, Hanley-Bowdoin L. 2011.
769 Functional Analysis of a Novel Motif Conserved across Geminivirus Rep Proteins. *J Virol*
770 85:1182–1192.

771 90. Varsani A, Krupovic M. 2017. Sequence-based taxonomic framework for the classification of
772 uncultured single-stranded DNA viruses of the family Genomoviridae. *Virus Evol* 3.

773 91. Shi M, Lin XD, Tian JH, Chen LJ, Chen X, Li CX, Qin XC, Li J, Cao JP, Eden JS, Buchmann J,
774 Wang W, Xu J, Holmes EC, Zhang YZ. 2016. Redefining the invertebrate RNA virosphere.
775 *Nature* 540:539–543.

776 92. Dolja V V., Koonin E V. 2018. Metagenomics reshapes the concepts of RNA virus evolution by
777 revealing extensive horizontal virus transfer. *Virus Res* 244:36–52.

778 93. Greninger AL, DeRisi JL. 2015. Draft Genome Sequence of Tombunodavirus UC1. *Genome*
779 *Announc* 3.

780 94. Krupovic M. 2013. Networks of evolutionary interactions underlying the polyphyletic origin of
781 ssDNA viruses. *Curr Opin Virol* 3:578–586.

782 95. Allison AB, Organtini LJ, Zhang S, Hafenstein SL, Holmes EC, Parrish CR. 2016. Single
783 Mutations in the VP2 300 Loop Region of the Three-Fold Spike of the Carnivore Parvovirus
784 Capsid Can Determine Host Range. *J Virol*.

785 96. Carbonell A, Maliogka VI, Pérez J de J, Salvador B, León DS, García JA, Simón-Mateo C. 2013.
786 Diverse Amino Acid Changes at Specific Positions in the N-Terminal Region of the Coat Protein
787 Allow Plum pox virus to Adapt to New Hosts. *Mol Plant-Microbe Interact* 26:1211–1224.

788 97. Beakes GW, Glockling SL, Sekimoto S. 2012. The evolutionary phylogeny of the oomycete
789 “fungi.” *Protoplasma* 249:3–19.

790 98. Hanyu N, Kuchino Y, Nishimura S, Beier H. 1986. Dramatic events in ciliate evolution: alteration
791 of UAA and UAG termination codons to glutamine codons due to anticodon mutations in two
792 Tetrahymena tRNAs Gln . *EMBO J* 5:1307–1311.

793 99. Soffer N, Brandt ME, Correa AMS, Smith TB, Thurber RV. 2014. Potential role of viruses in
794 white plague coral disease. *ISME J* 8:271–283.

795 100. Krupovic M, Bamford DH. 2010. Order to the Viral Universe. *J Virol* 84:12476–12479.

Figure 1

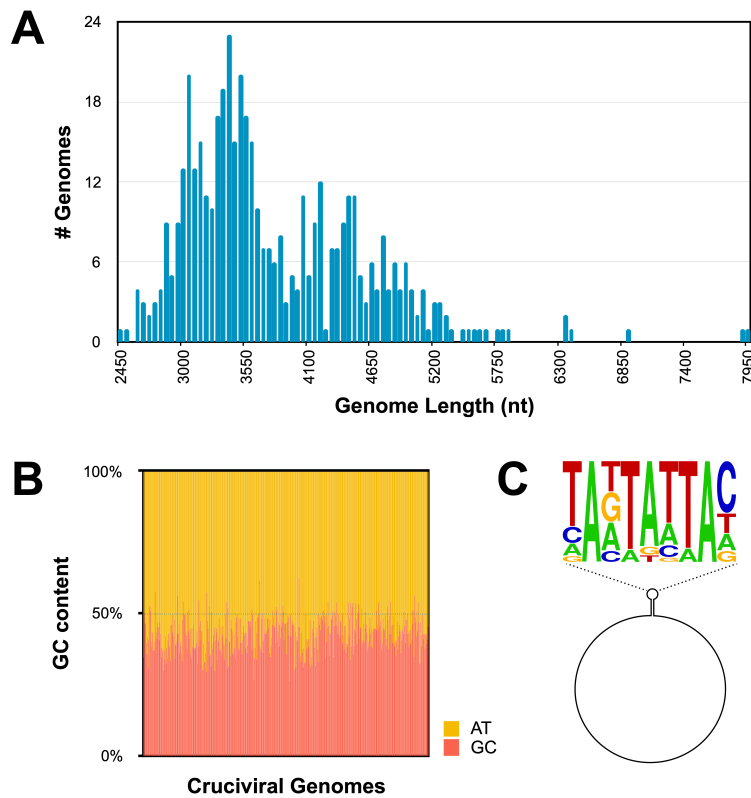


Figure 1. Genome properties of 461 new cruciviral circular sequences. (A) Histogram of cruciviral genome lengths categorized in 50 nt bins. **(B)** Percentage of G + C content versus A + T in each of the sequences described in this study **(C)** Relative abundance of nucleotides in the conserved nonanucleotide sequence of the 211 stem-loops and putative origins of replication represented predicted with StemLoop-Finder (Pratt *et al.*, unpublished) in Sequence Logo format.

Figure 2

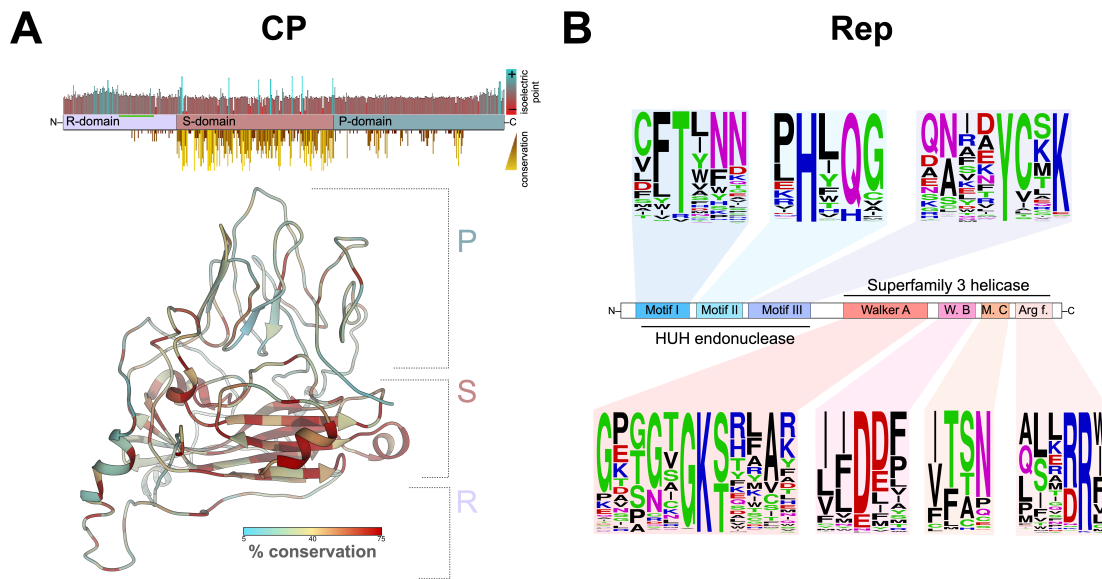


Figure 2. Protein conservation in cruciviruses. **(A)** **Top:** distribution of domains, isoelectric point and conservation in a consensus capsid protein (CP). 461 CP protein sequences were aligned in Geneious 11.0.4 with MAFFT (G-INS-i, BLOSUM 45, open gap penalty 1.53, offset 0.123) and trimmed manually. The conservation of the physico-chemical properties at each position was obtained with Jalview v2.11.0, and the isoelectric point was estimated in Geneious 11.0.4. The region of CP rich in glycine is highlighted with a green bar. **Bottom:** Structure of a cruciviral CP (CruV-359) as predicted by Phyre² showing sequence conservation based on an alignment of the 47 CP protein sequences from the CP-based clusters. **(B)** Conserved motifs found in cruciviral Reps after aligning all the extracted Rep protein sequences using PSI-Coffee. Sequence logos were generated at <http://weblogo.threplusone.com> to indicate the frequency of residues at each position.

Figure 3

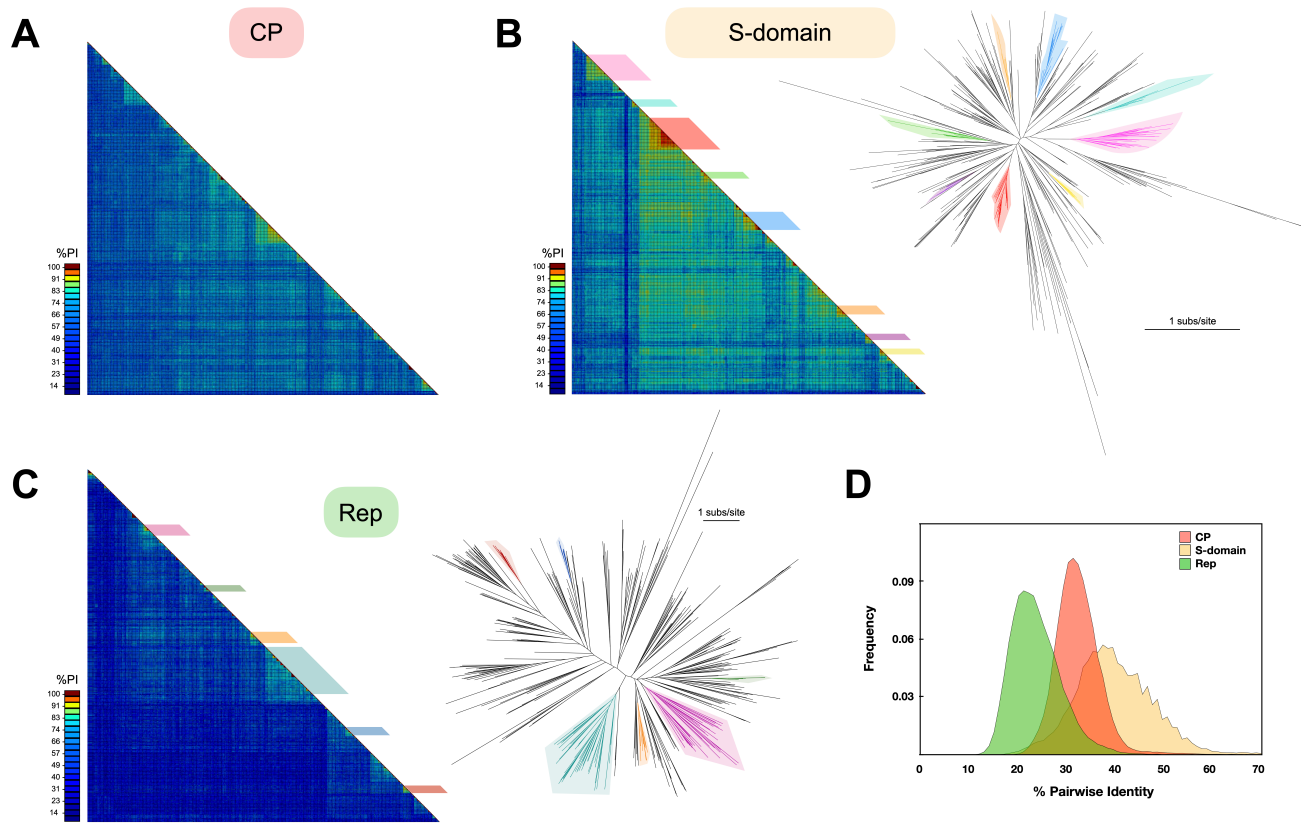


Figure 3. Diversity of cruciviral proteins. **(A) CP diversity.** Pairwise amino acid identity (PI) between the CPs predicted for 461 cruciviral sequences. The alignment and analysis were carried out with SDT, using the integrated MAFFT algorithm. **(B) S-domain diversity.** **Left:** PI matrix between the capsid protein (CP) predicted S-domain of the 461 sequences described in this study. The alignment and analysis were carried out with SDT, using the integrated MAFFT algorithm. The colored boxes indicate the different clusters of sequences used to create the CP-based clusters sequence subset. **Right:** Unrooted phylogenetic tree obtained with FastTree from a manually curated MAFFT alignment of the translated sequences of the S-domain (G-INS-i, BLOSUM 45, open gap penalty 1.53, offset 0.123). The colored branches represent the different clusters observed in the matrix. Scale bar indicates substitutions per site. **(C) Rep diversity.** **Left:** Pairwise identity (PI) matrix between all Reps found in cruciviral genomes in this study. The alignment and analysis were carried out with SDT, using the integrated MUSCLE algorithm. **Right:** Unrooted phylogenetic tree obtained with FastTree from an PSI-Coffee alignment of the translated sequences of Rep trimmed with TrimAl v1.3. The colored branches represent the different clusters that contain *Rep-based clusters* sequence subset. Scale bar indicates substitutions per site. **(D) PI frequency distribution.** The frequency of PI values for each of the putative proteins or domains analyzed is shown.

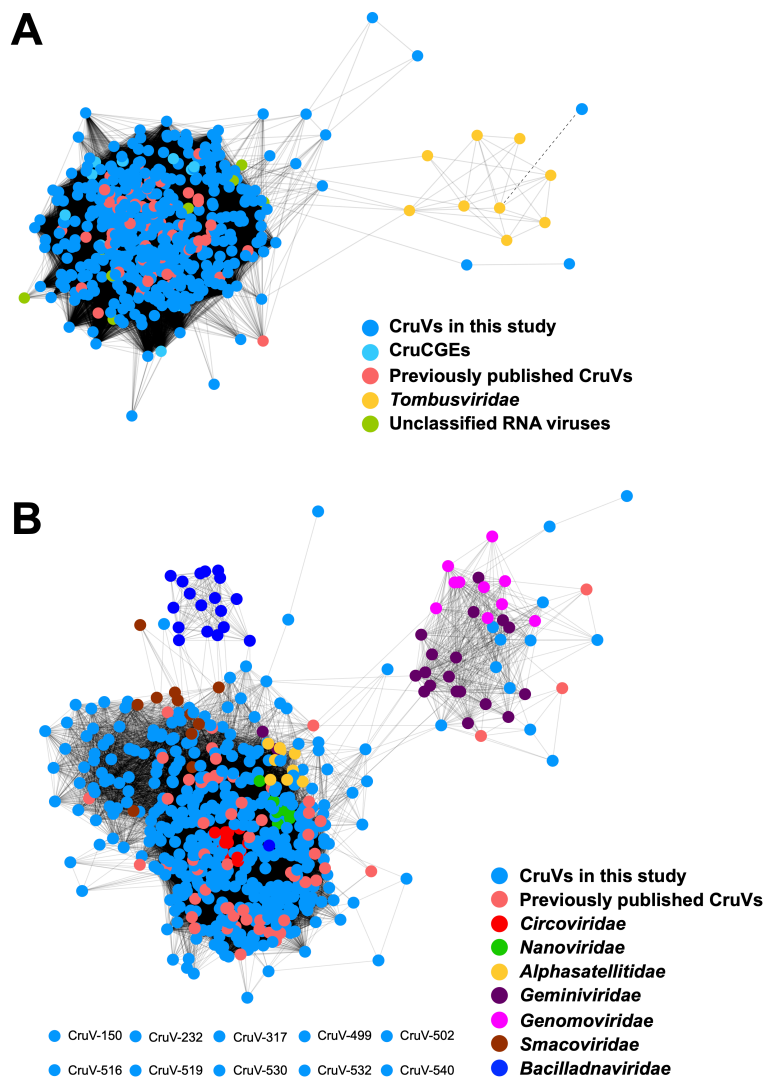
Figure 4

Figure 4. Similarity networks of cruciviral proteins with related viruses. **(A)** Capsid proteins (CP) represented by colored dots are connected with a solid line when the similarity between them is greater than $e\text{-value}=1\text{e}^{-20}$. The dashed line represents an $e\text{-value} = 6\text{e}^{-7}$ between the nodes corresponding to the CP of CruV-523 and turnip crinkle virus, as given by BLASTp. **(B)** Replication-associated protein (Rep) translations, represented by colored dots, are connected with a solid line when the similarity between them greater than $e\text{-value}=1\text{e}^{-10}$. The eight nodes at the bottom left did not connect to any other node. All networks were carried out with pairwise identities calculated in the EFI-EST web server and visualized in Cytoscape v3.7.2.

Figure 5

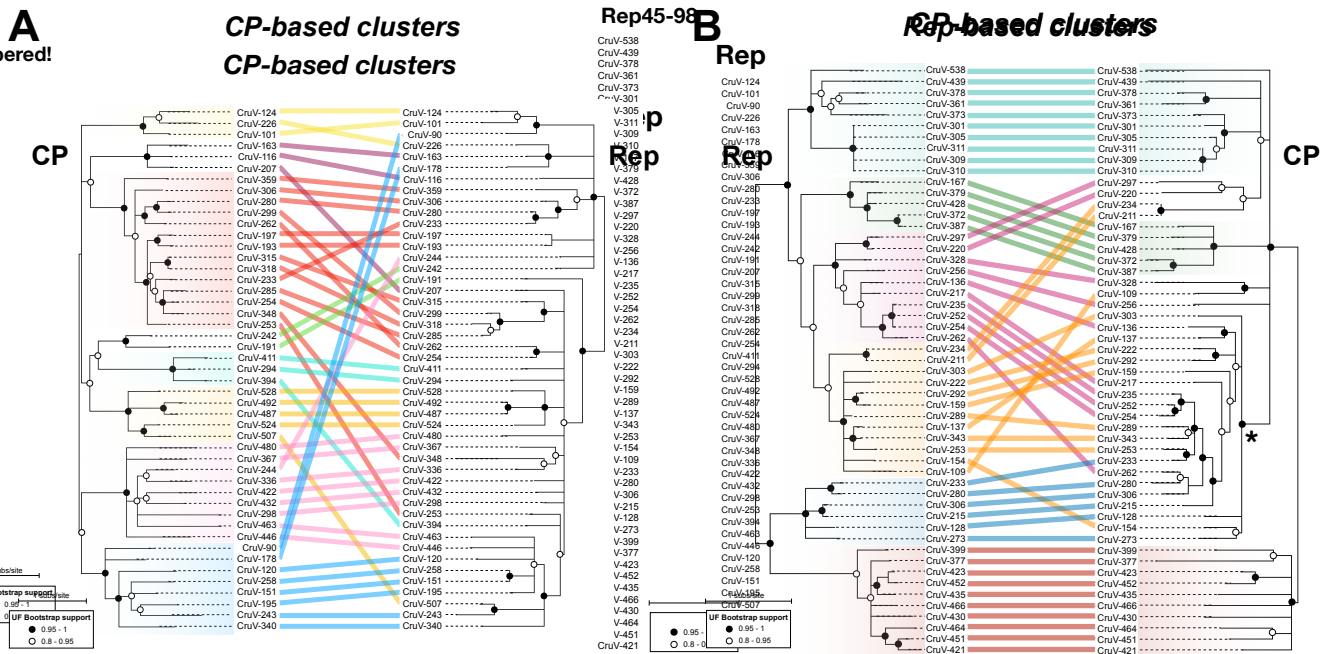


Figure 5. Comparison of phylogenies of CP and Rep proteins of representative cruciviruses. (A) Tanglegram calculated with Dendroscope v3.5.10 from phylogenetic trees generated with PhyML from Cp (PhyML automatic model selection LG+G+I+F) and Rep (PhyML automatic model selection RtREV+G+I) alignments. The tips corresponding to the same viral genome are linked by lines that are color-coded according to the clusters obtained from Fig. 3A (CP-based clusters). **(B)** Tanglegram calculated with Dendroscope v3.5.10 from phylogenetic trees generated with PhyML from Cp (PhyML automatic model selection LG+G+I+F) and Rep (PhyML automatic model selection RtREV+G+I) alignments. The tips corresponding to the same viral sequence are linked by lines that are color-coded according to the clusters obtained from Fig. 3B (Rep-based clusters). The clade marked with an asterisk is formed by members of the red cluster of subset A. Branch support is given according to aLRT SH-like (Anisimova & Gascuel, 2006). All nodes with an aLRT SH-like branch support inferior to 0.8 were collapsed with Dendroscope prior to constructing the tanglegram.

Figure 6

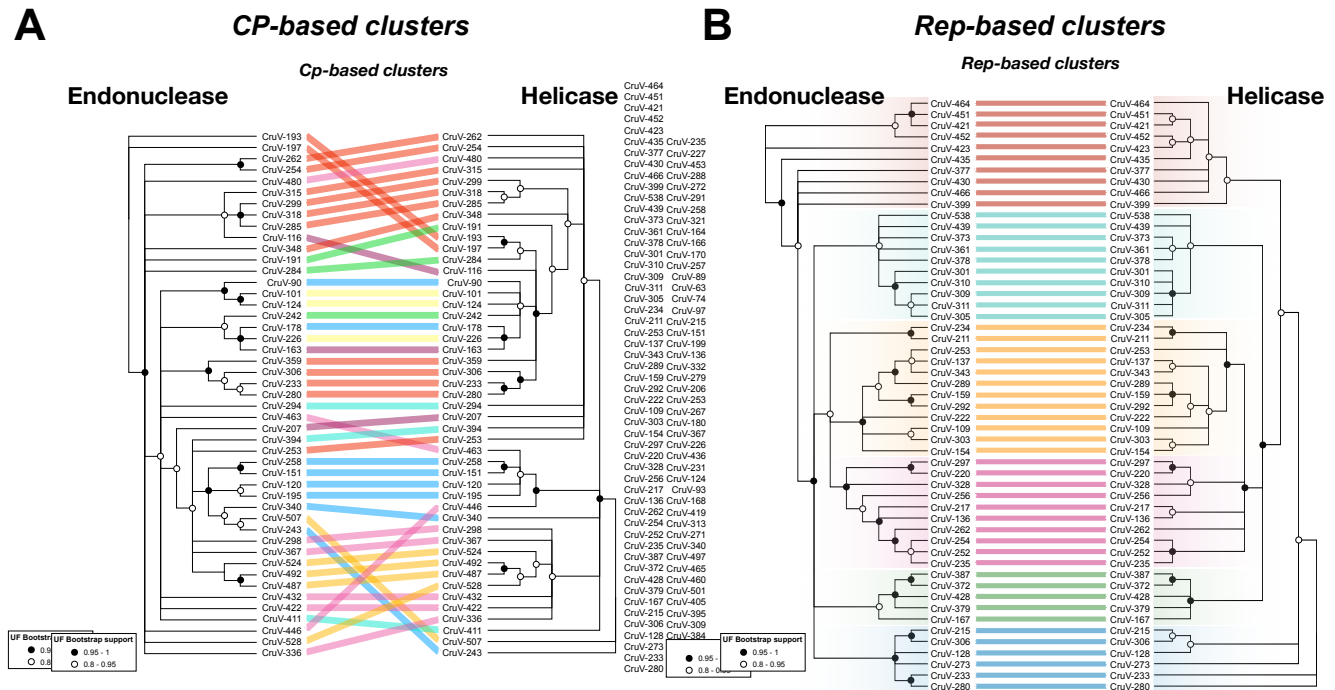


Figure 6. Comparison of phylogenies between the endonuclease and helicase domains of Reps from representative cruciviruses. (A) Tanglegram calculated with Dendroscope v3.5.10 from phylogenetic trees generated with PhyML from separate alignments of Rep endonuclease and helicase domains. The tips corresponding to the same viral genome are linked by lines that are color-coded according to the clusters obtained from Fig. 3A (CP-based clusters). (B) Same as A but with sequences from the clusters obtained from Fig. 3B (Rep-based clusters). All nodes with an aLRT SH-like branch support inferior to 0.8 were collapsed with Dendroscope v3.5.10 prior to constructing the tanglegram.